Gross appearance of brain tumors

Gross appearance of brain tumors are presented. The complaints are primarily due to mass effects, including seizures, focal effects and headache. The majority of adult primary tumors are supratentorial, while the majority of childhood primary tumors are infratentorial. Enjoy the journey of brain tumors.

Ref.: Stoyanov GS, et al. A practical approach to the differential diagnosis of intracranial tumors: Ggoss, histology, and immunoprofile-based algorithm. Cureus 2019; 11(12): e6384. doi: 10.7759/cureus.6384

Rathke’s sinus

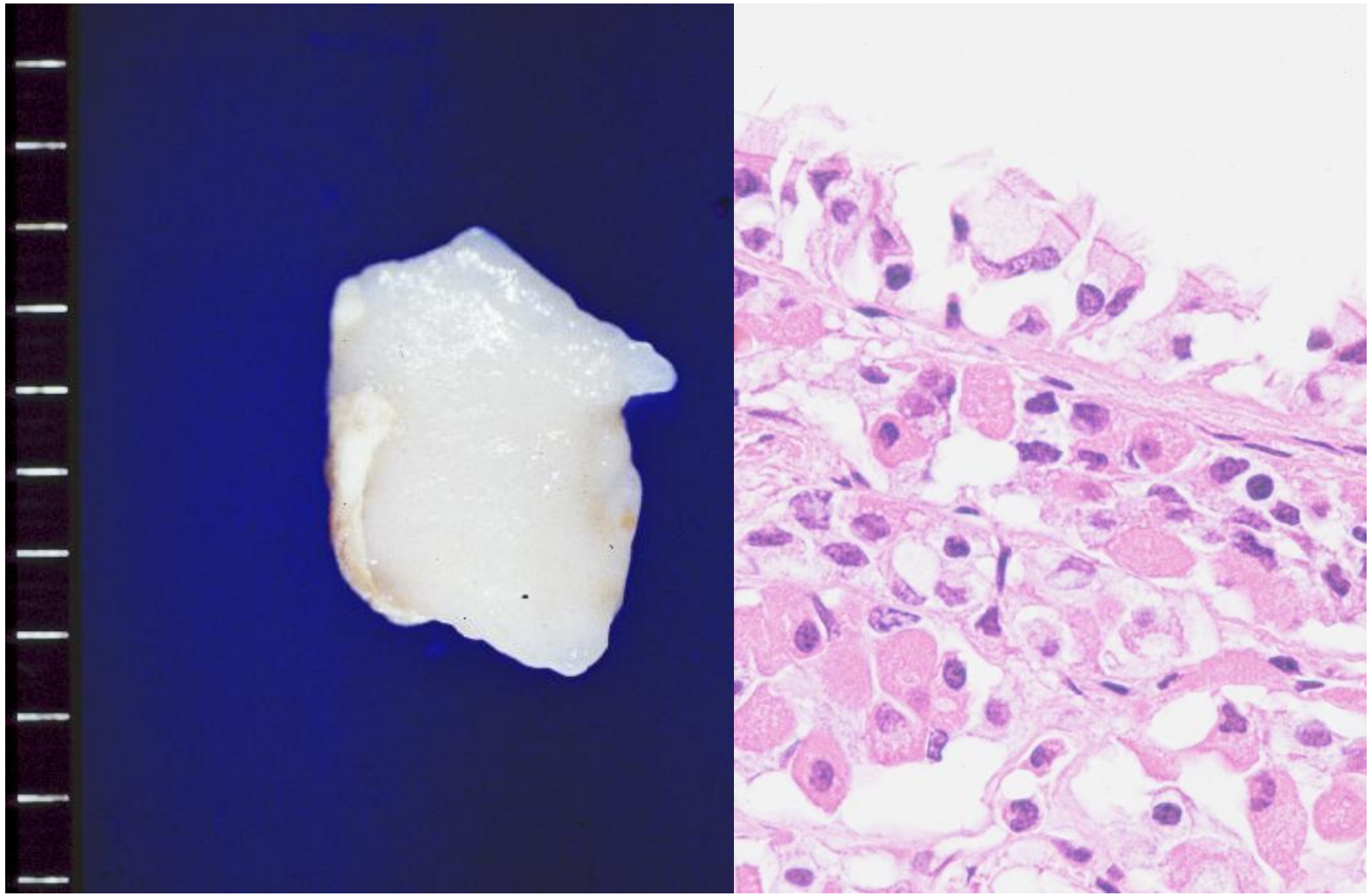

A Rathke’s cyst located at the infundibulum of a 15-year-old boy. A 25 mm-sized cyst (left: gross appearance) is microscopically lined by ciliated columnar cells seen just adjacent to the anterior pituitary gland (right: H&E).

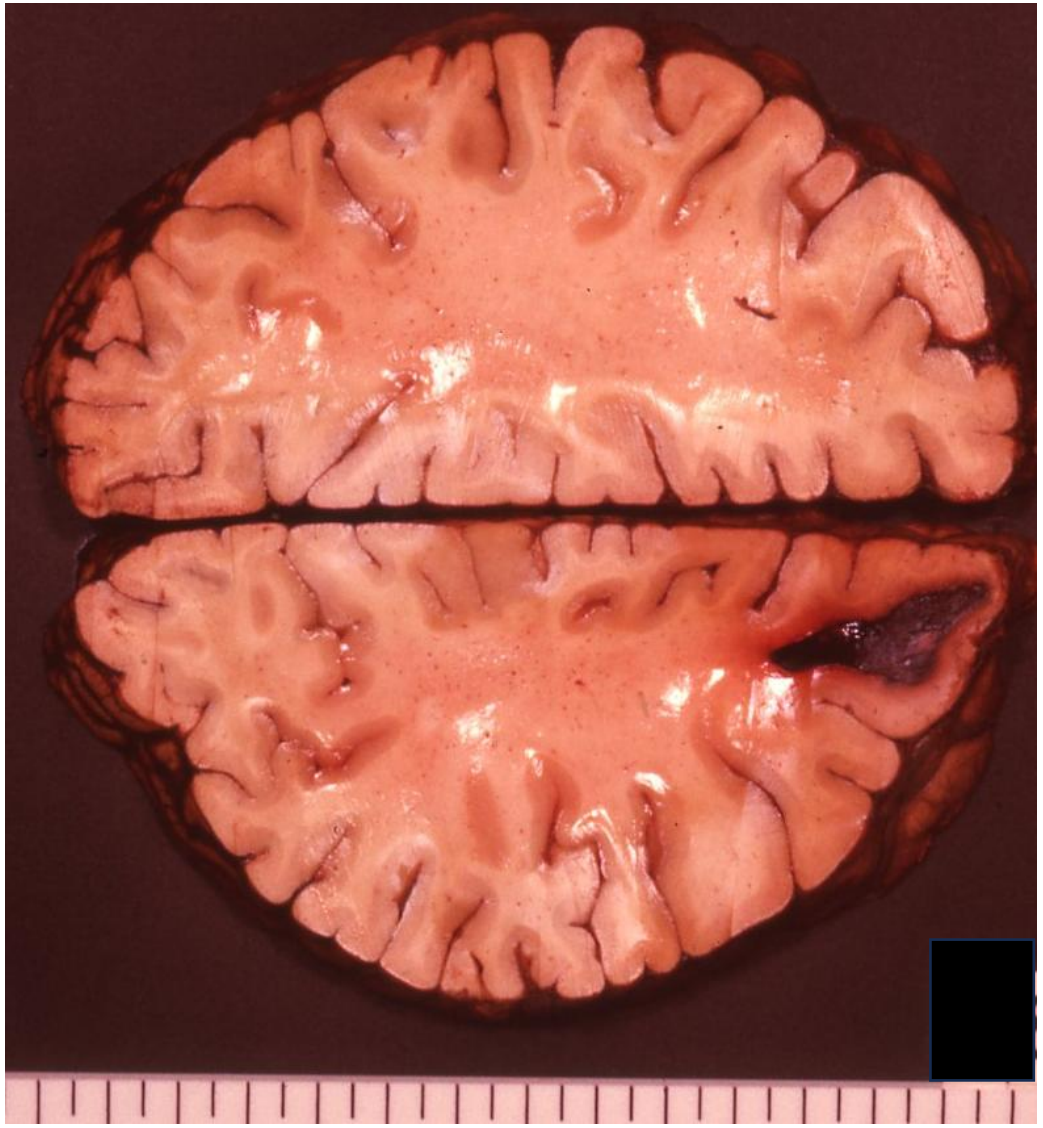

Cavernous hemangioma of the white matter of the left frontal lobe. A 50-year-old male patient.

Diffuse astrocytoma of the brain stem in children (a sagittal section).
The mid brain through the medulla oblongata are diffusely infiltrated by the invasive tumor.

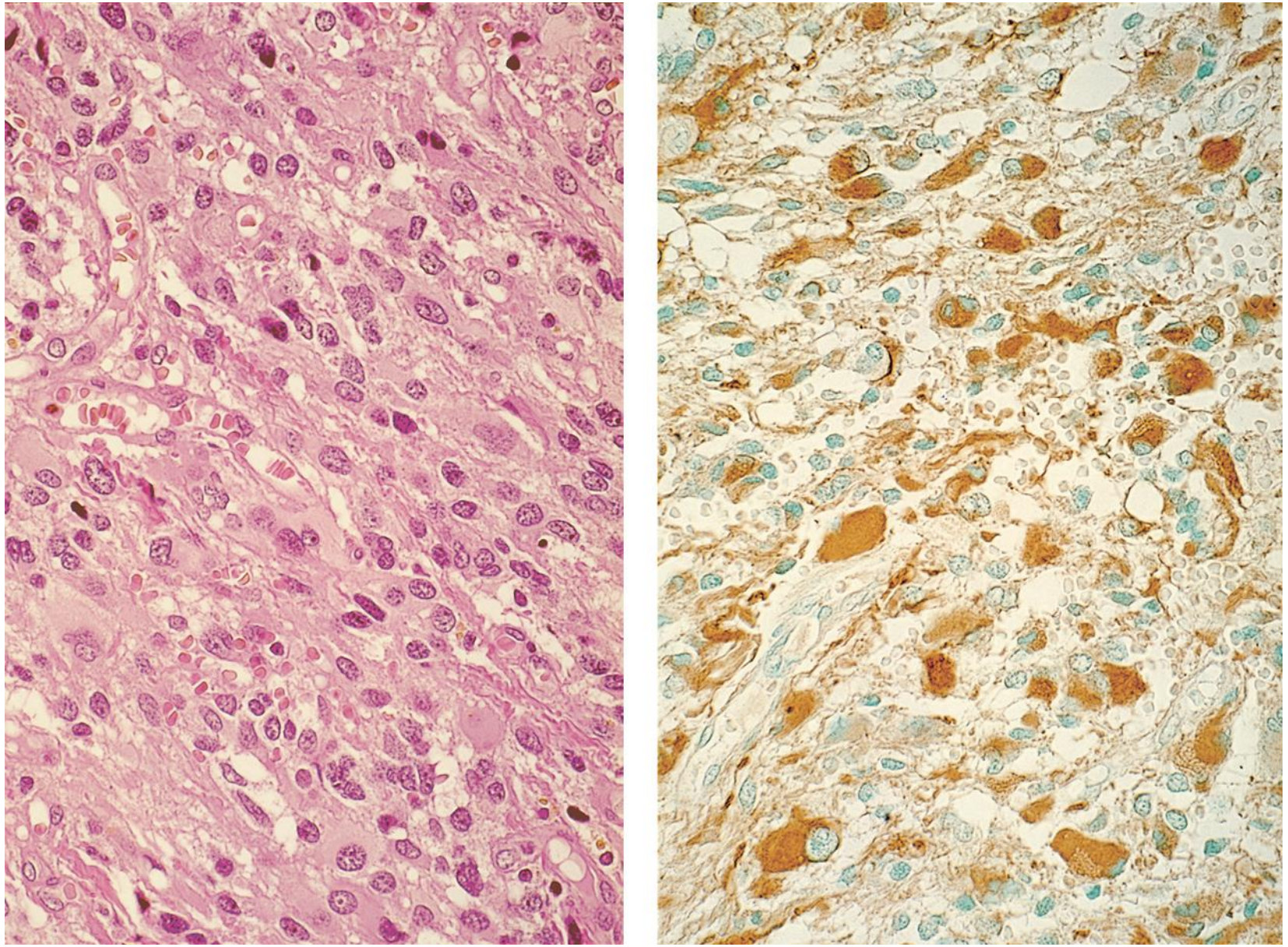

Microscopic appearance of diffuse astrocytoma of the brain stem (left: H&E, right: immunostaining for GFAP). Mildly pleomorphic astrocytes infiltrate the pontine tissue.

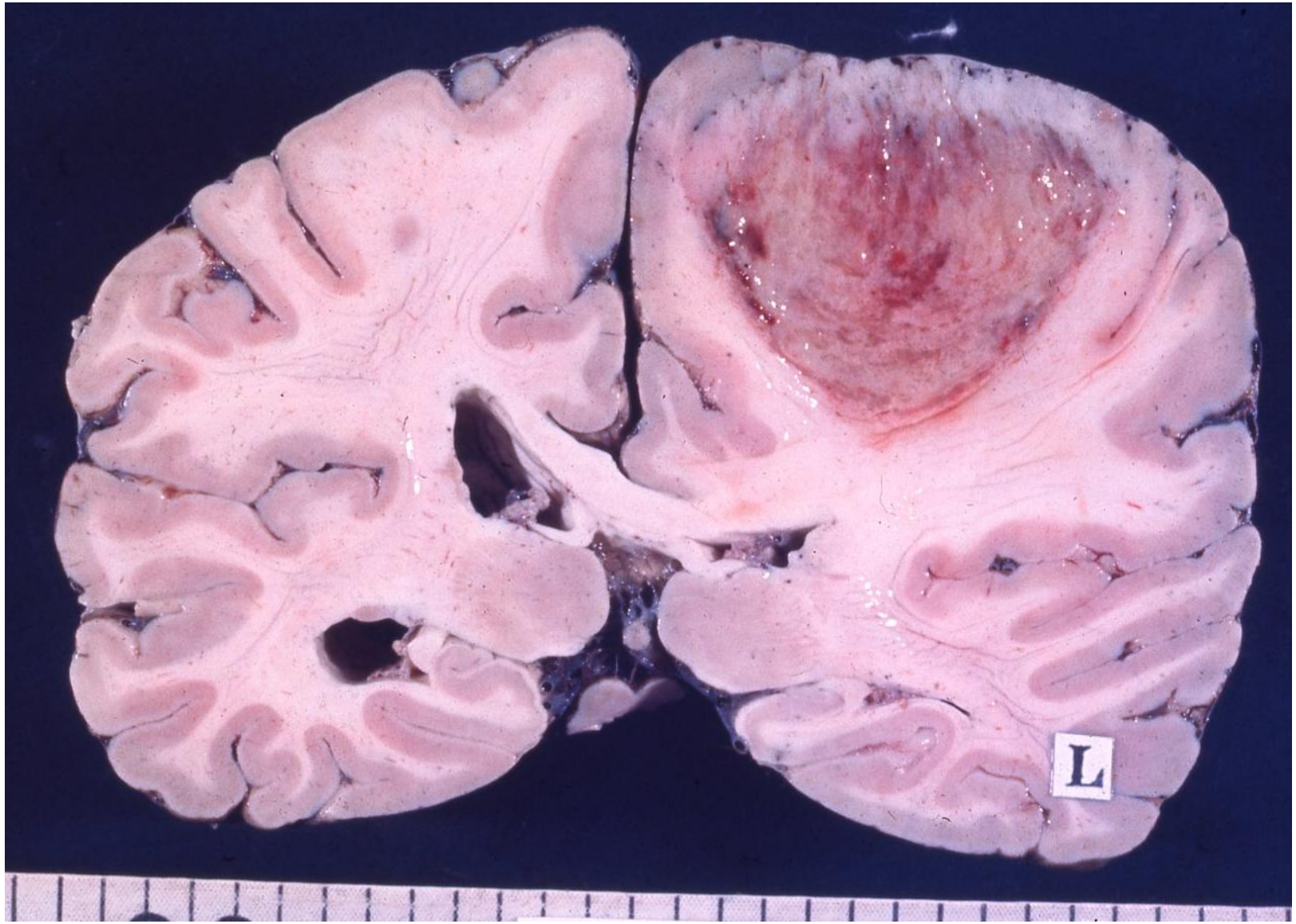

Glioblastoma multiforme in the left parietal lobe in a male patient aged 70’s. A 52 mm-sized tumor with multifocal necrosis occupies the white matter of the left parietal lobe. Cingulate herniation is associated.

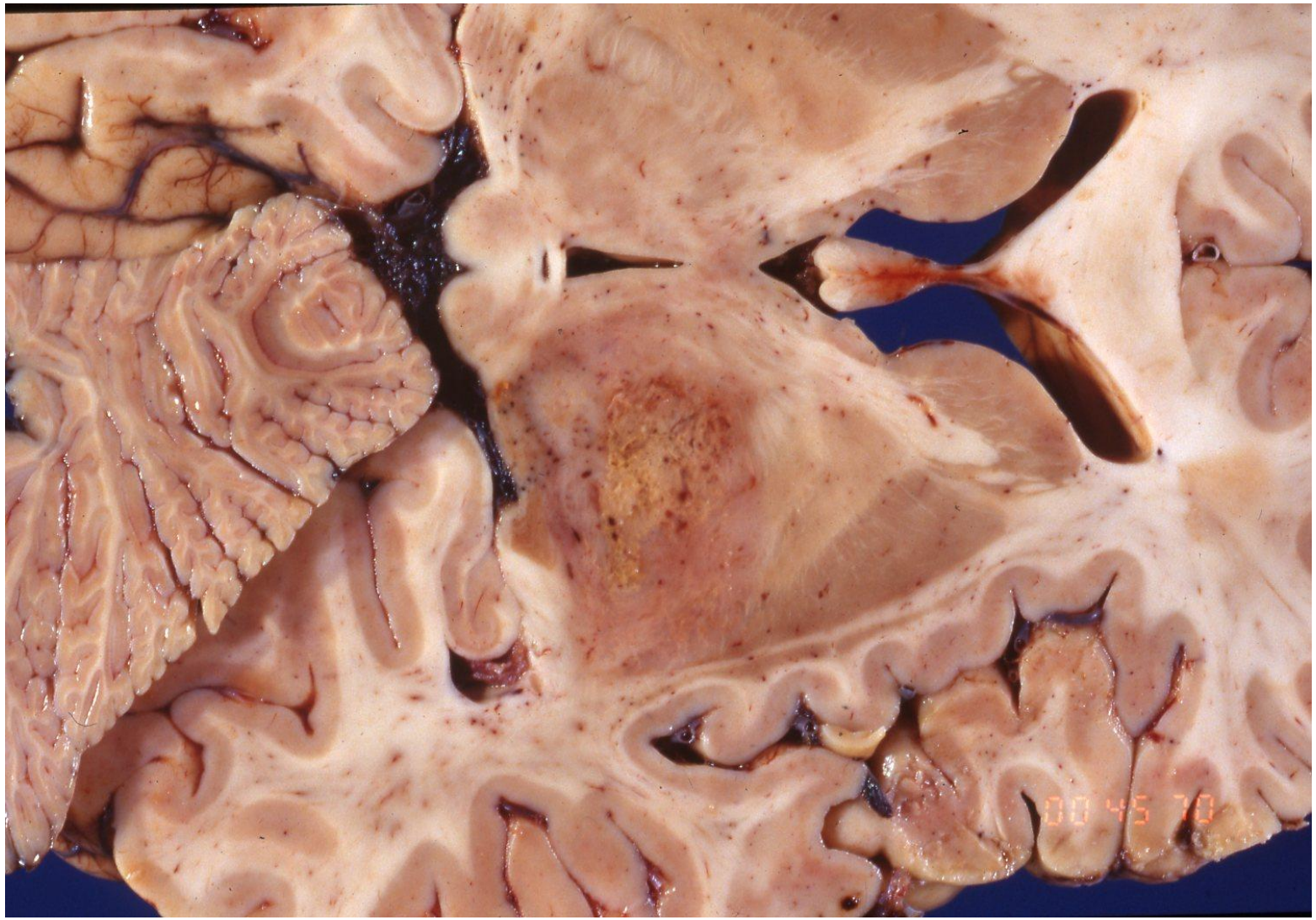

Anaplastic astrocytoma of the left thalamus of a 59-year-old female patient. An ill-defined infiltrative tumor with multifocal hemorrhagic necrosis is seen in the left thalamus.

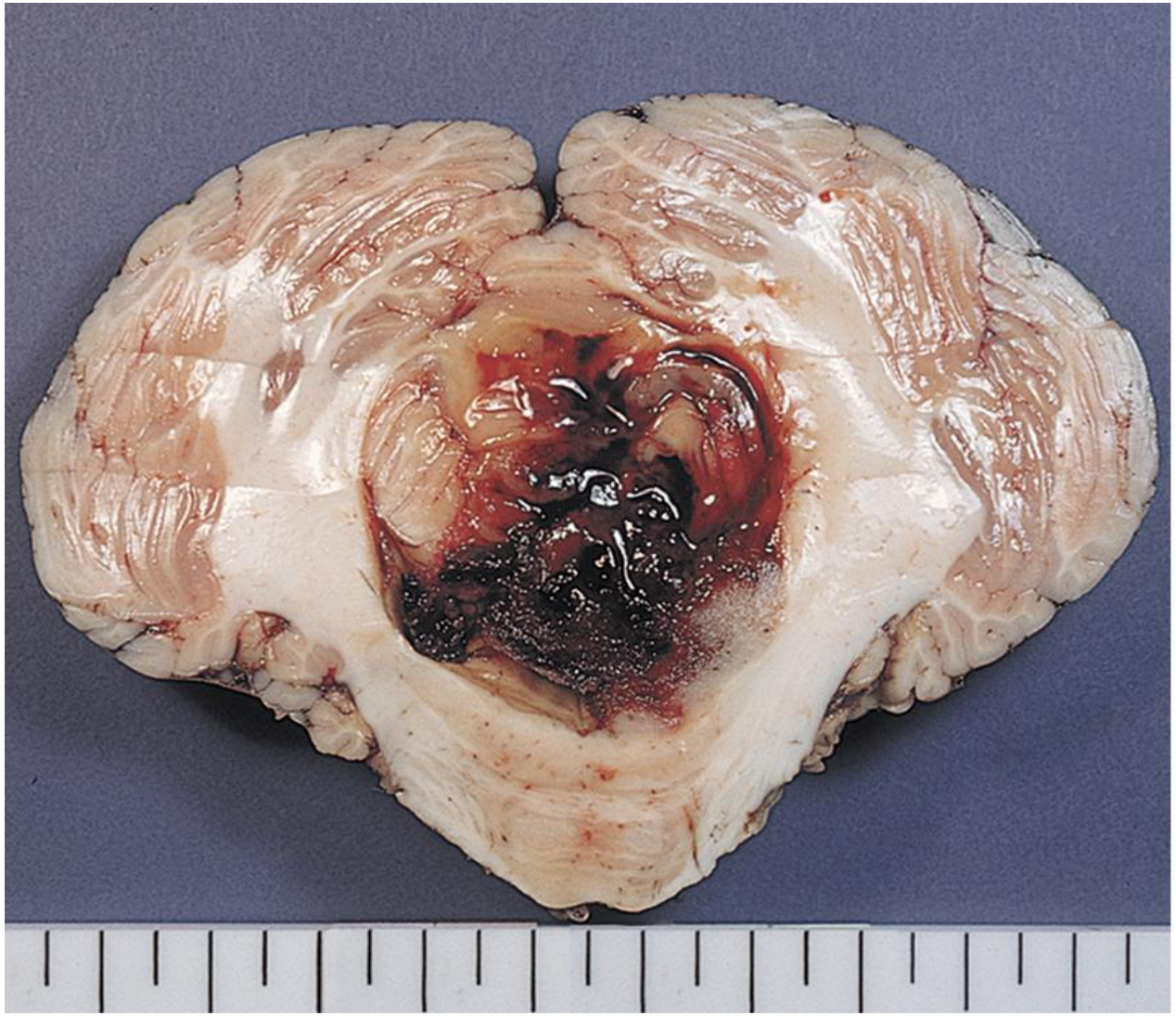

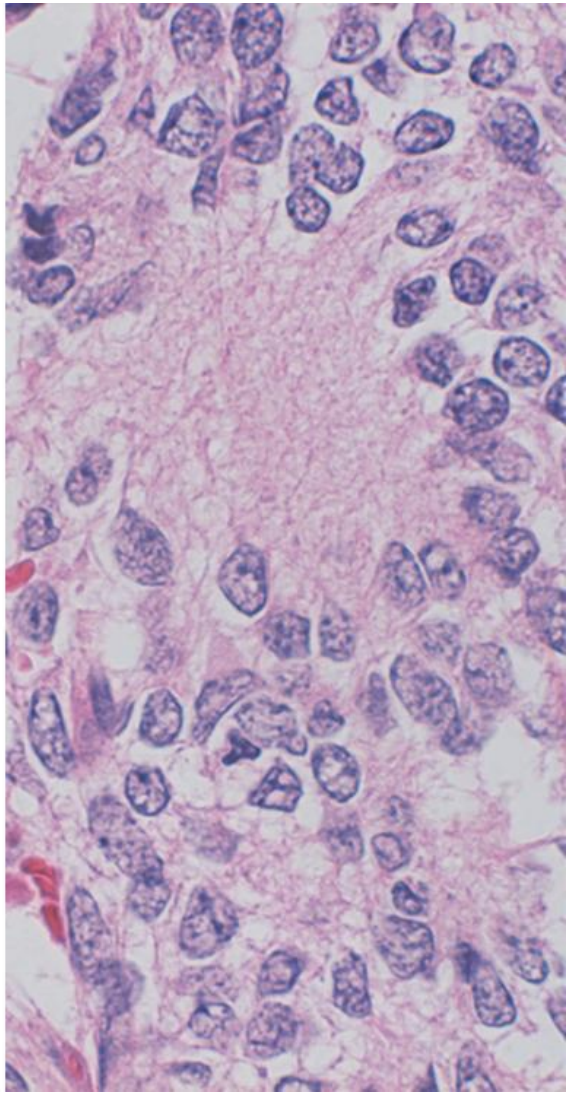

Medulloblastoma of the cerebellar vermis of a 9-year-old girl. A hemorrhagic tumor occupies the cerebellar vermis and the fourth ventricle. Rosette formation by small-sized neuroblasts is seen in H&E preparation (right).

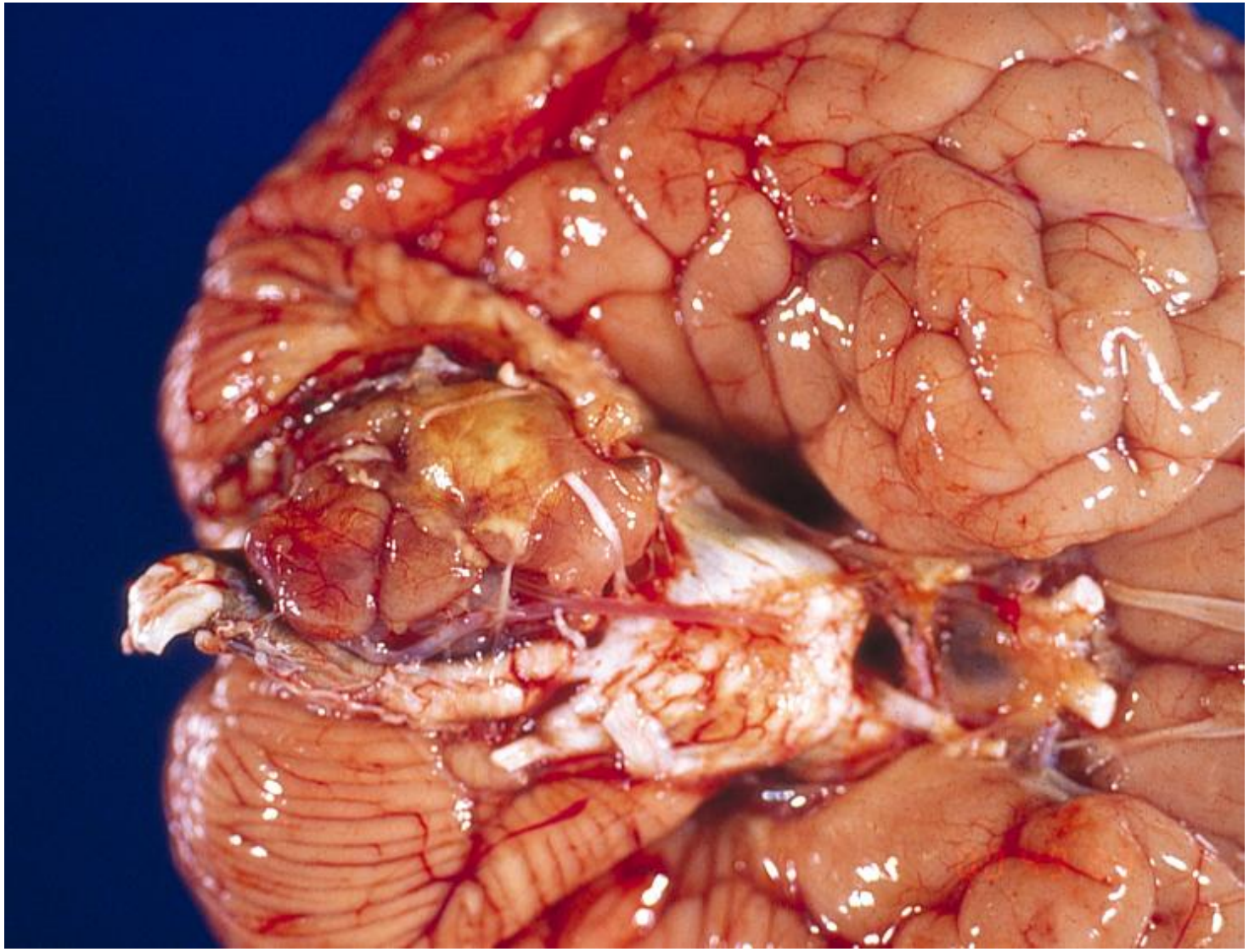

Ependymoma of the fourth ventricle of a 2-year-old boy (1). A focally necrotic mass is seen in the right-sided fourth ventricle, compressing the medulla oblongata.

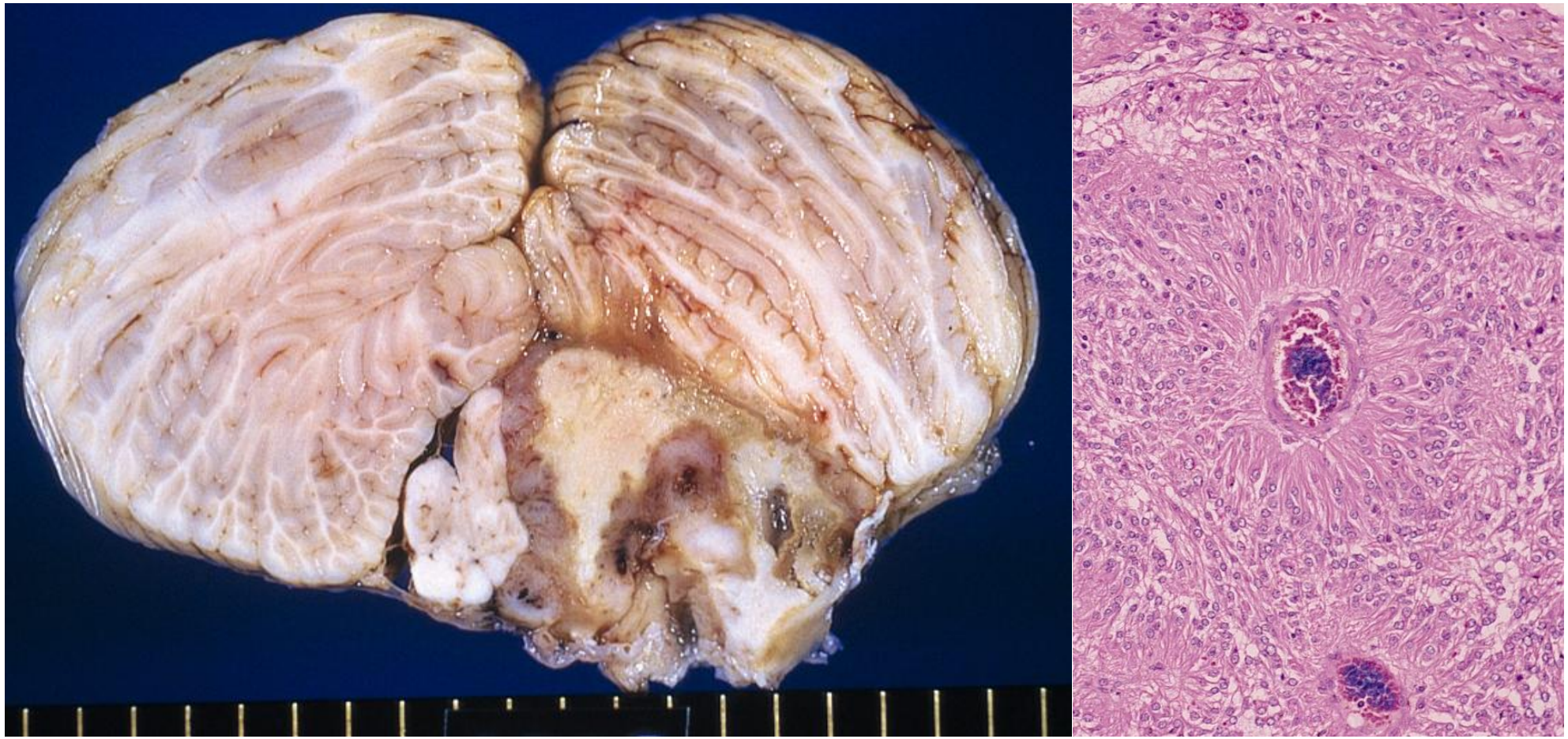

Ependymoma of the fourth ventricle of a 2-year-old boy (2). A hemorrhagic invasive mass is seen in the right-sided fourth ventricle, invading and destroying the medulla oblongata. Microscopically, perivascular pseudorosettes are formed (right: H&E).

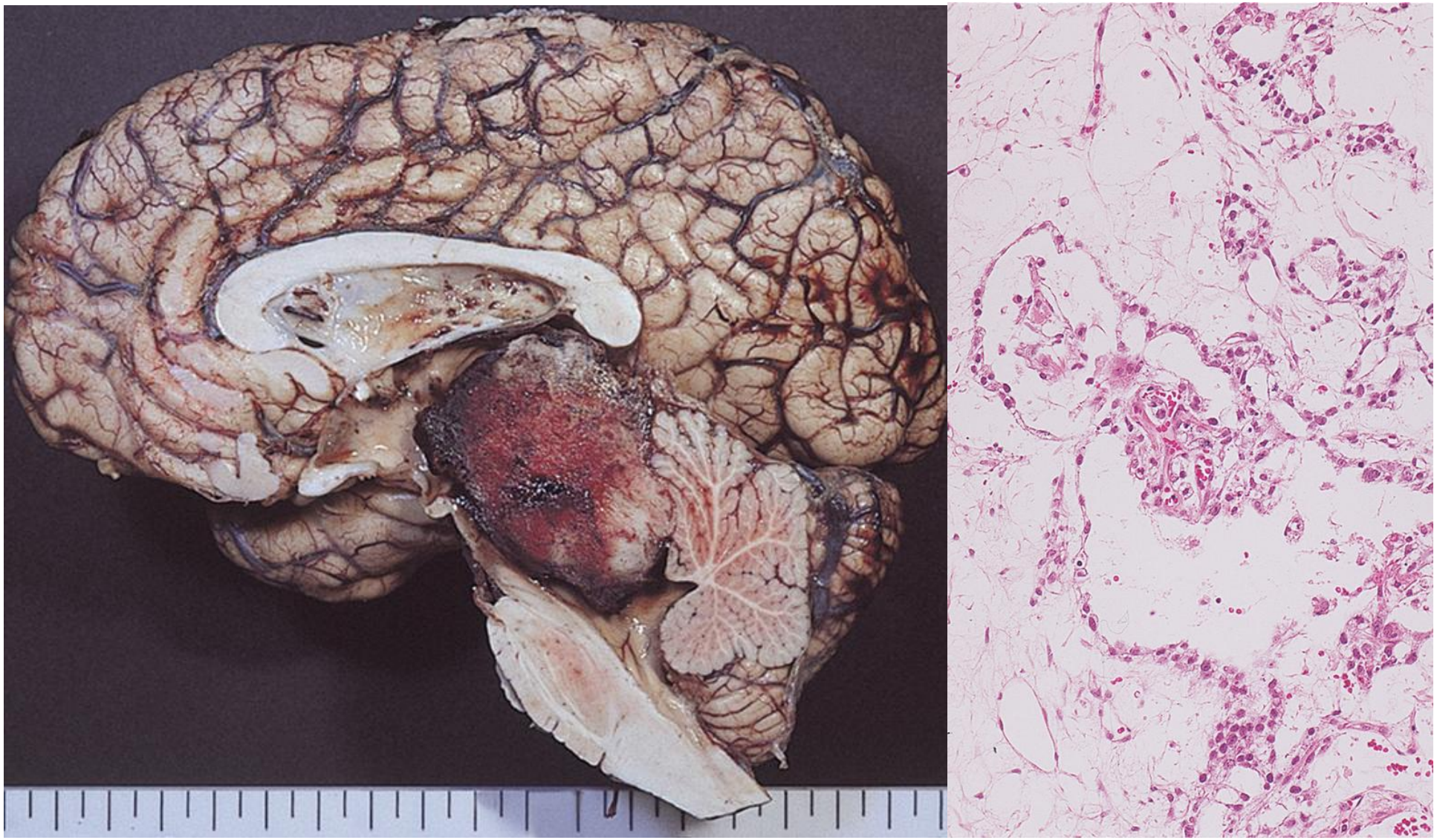

An AFP-producing yolk sac tumor of the pineal region seen in a 38-year-old male patient (a sagittal section). A hemorrhagic tumor, 50 x 45 mm in size, occupies the posterior part of the third ventricle. Microscopic features of yolk sac tumor are confirmed (right: H&E).

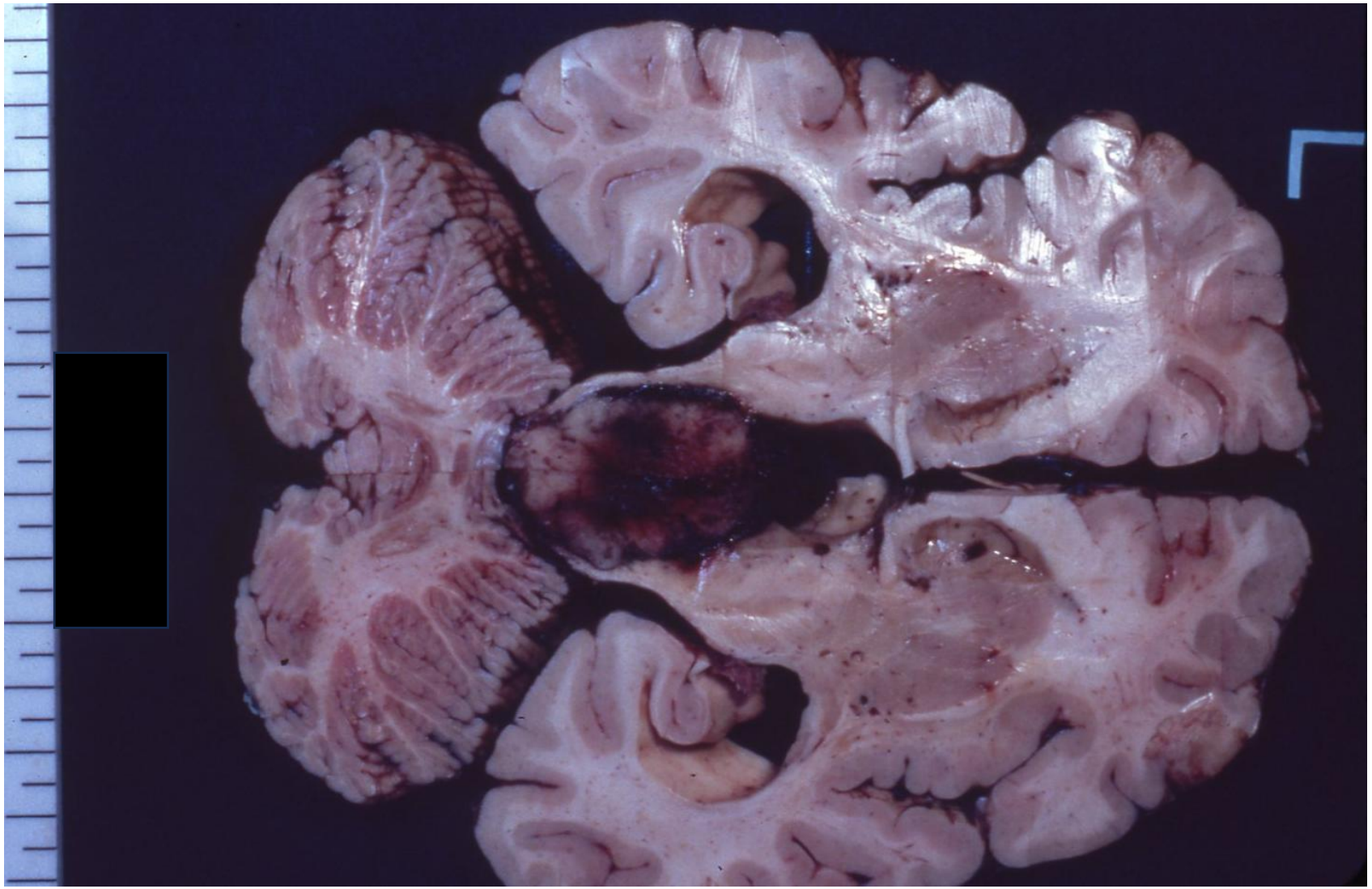

An AFP-producing yolk sac tumor of the pineal region seen in a 38-year-old male patient (a horizontal section). A hemorrhagic tumor, 50 x 45 mm in size, occupies the posterior part of the third ventricle.

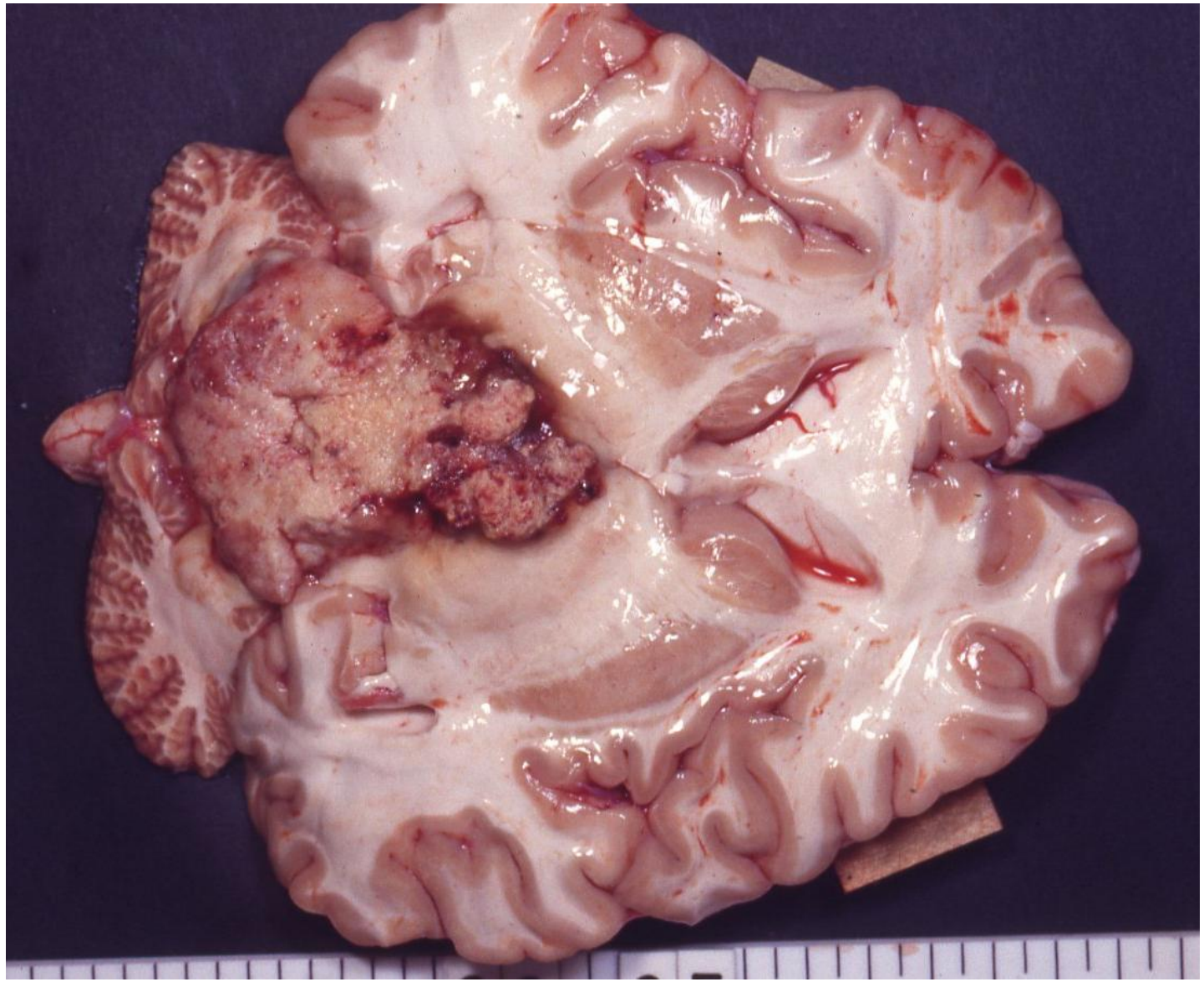

Another case of AFP-producing yolk sac tumor of the pineal region of a 20-year-old male patient is shown. An 80 x 70 mm necrotic tumor occupies the pineal region.

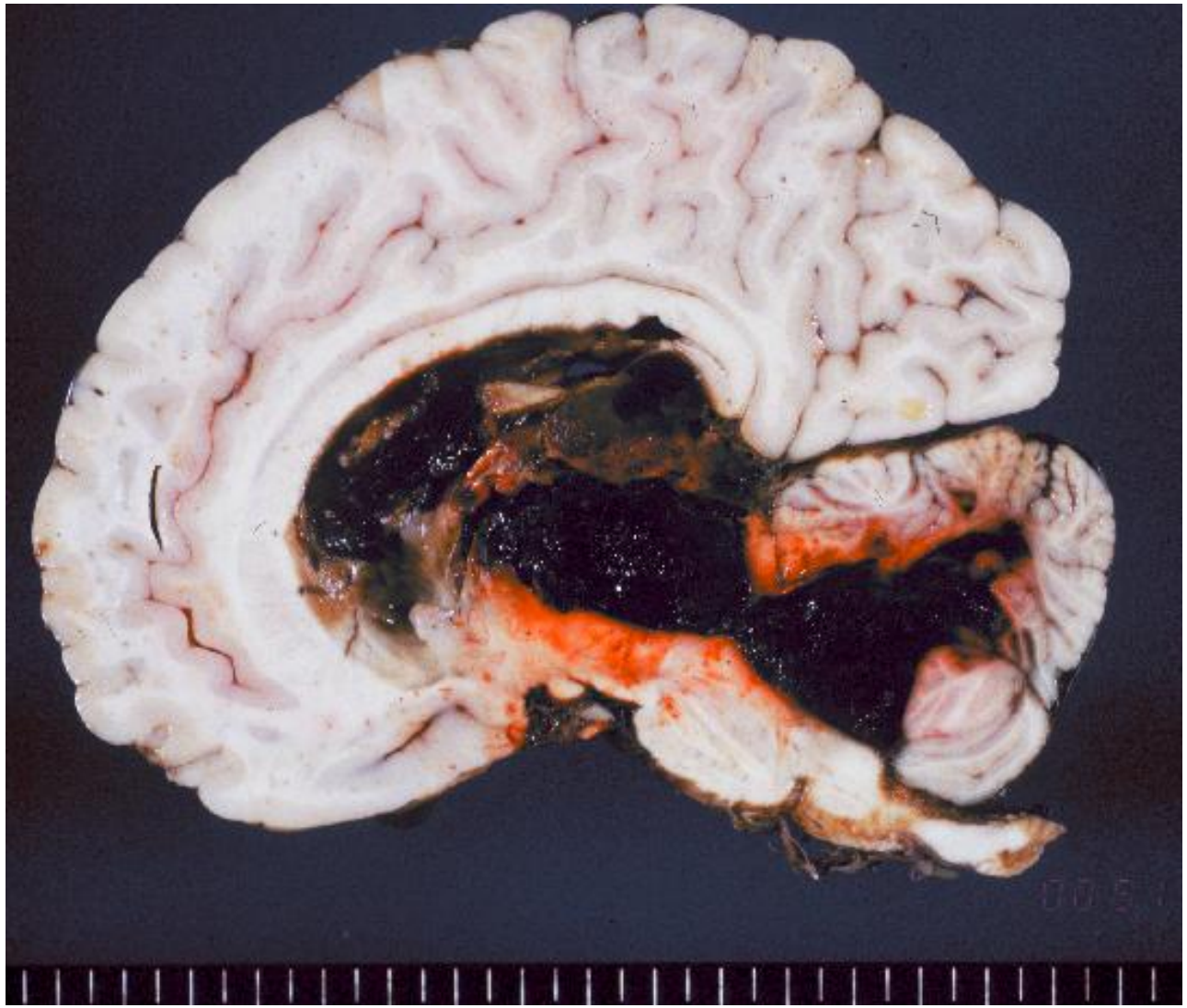

Choriocarcinoma of the pineal region of a 15-year-old boy. A massively hemorrhagic and invasive tumor occupies the pineal region. Hemorrhage into the third and fourth ventricles is associated (the direct cause of death). The HCG levels: 13,869 IU/L in the serum and 2,543 IU/L in the cerebrospinal fluid

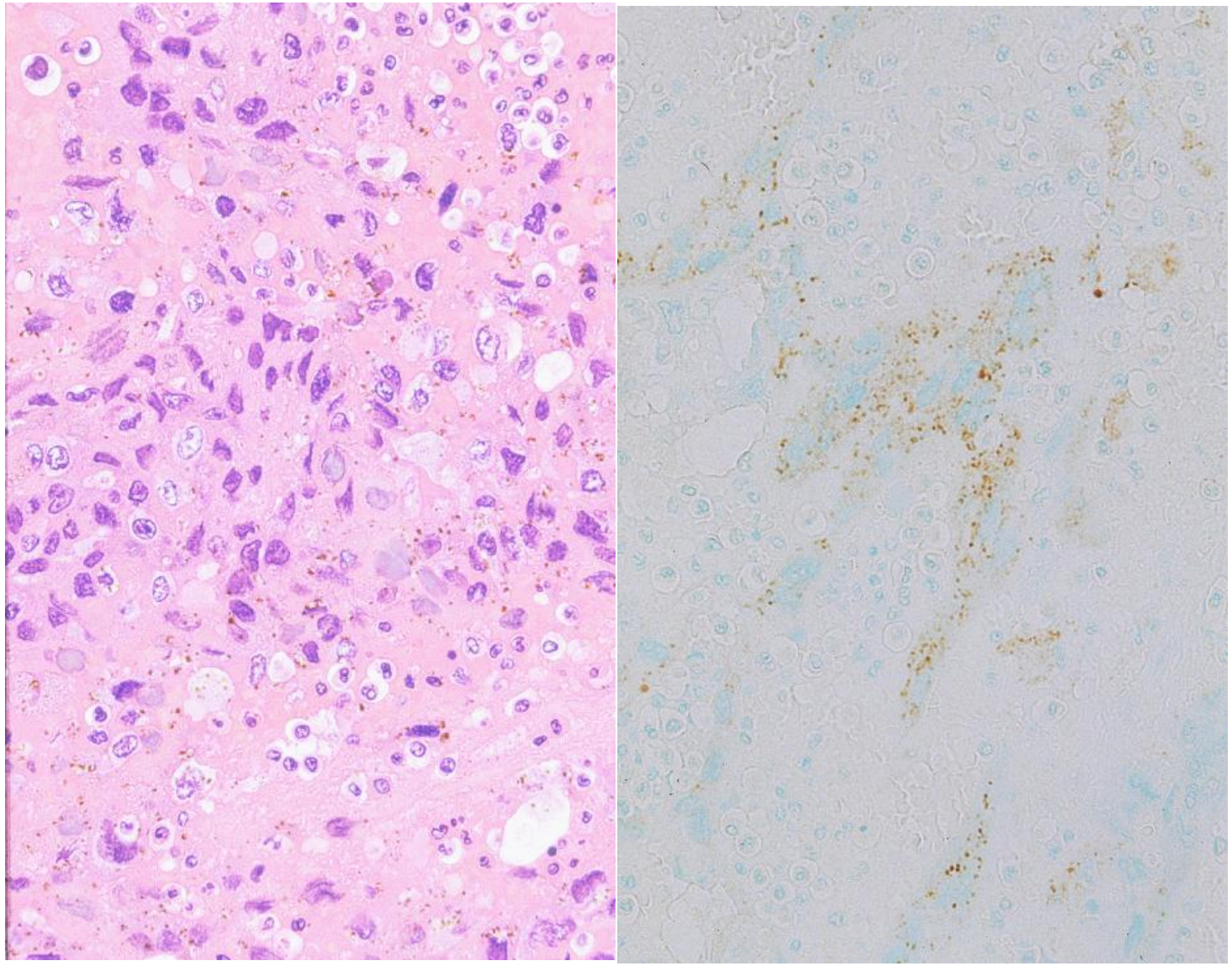

Choriocarcinoma of the pineal region of a 15-year-old boy. Microscopically, large-sized hyperchromatic tumor cells (left: H&E) are immunoreactive for HCG (right: immunostaining for HCG).

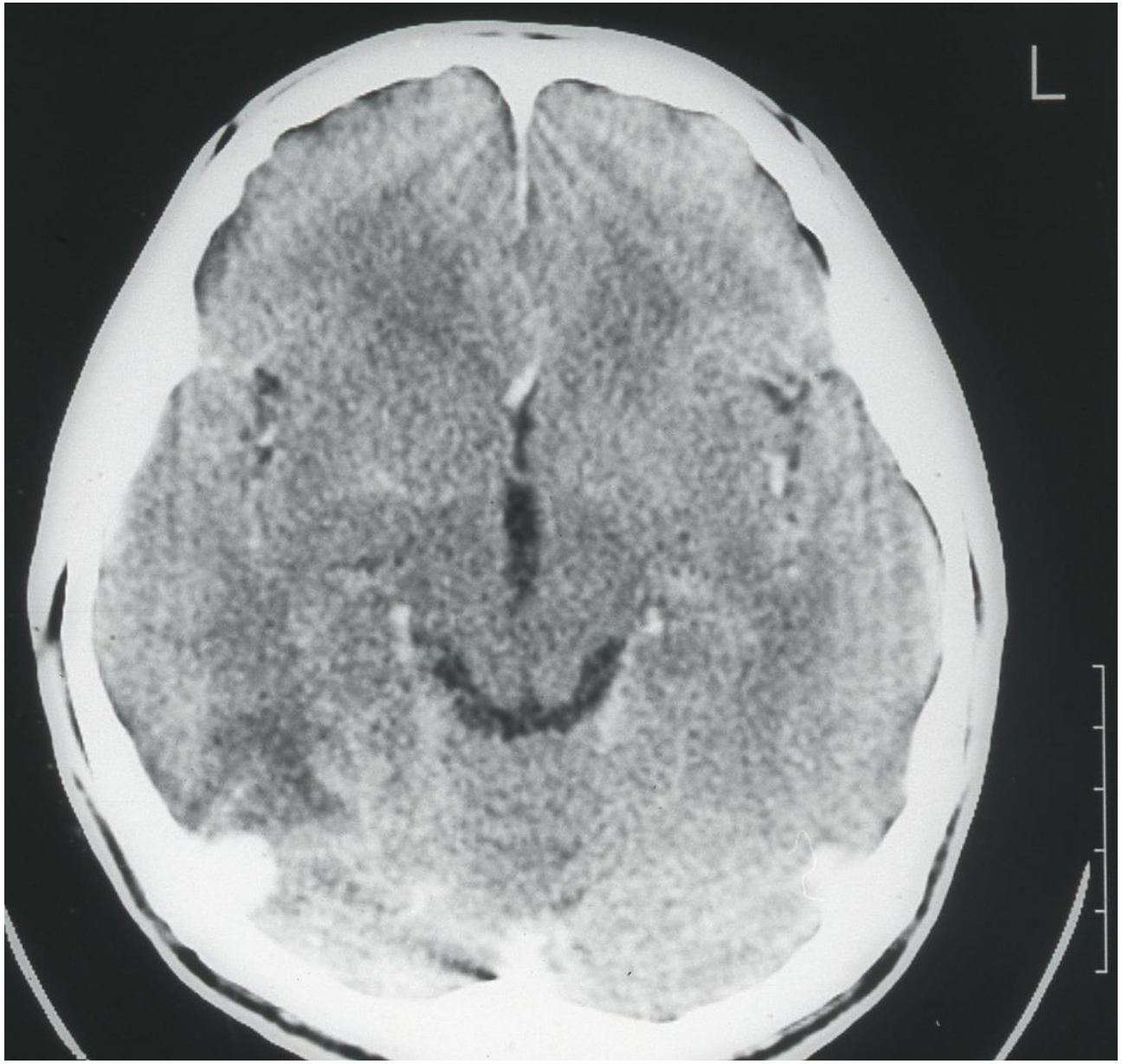

CT image of benign meningioma located at the right posterior lobe.

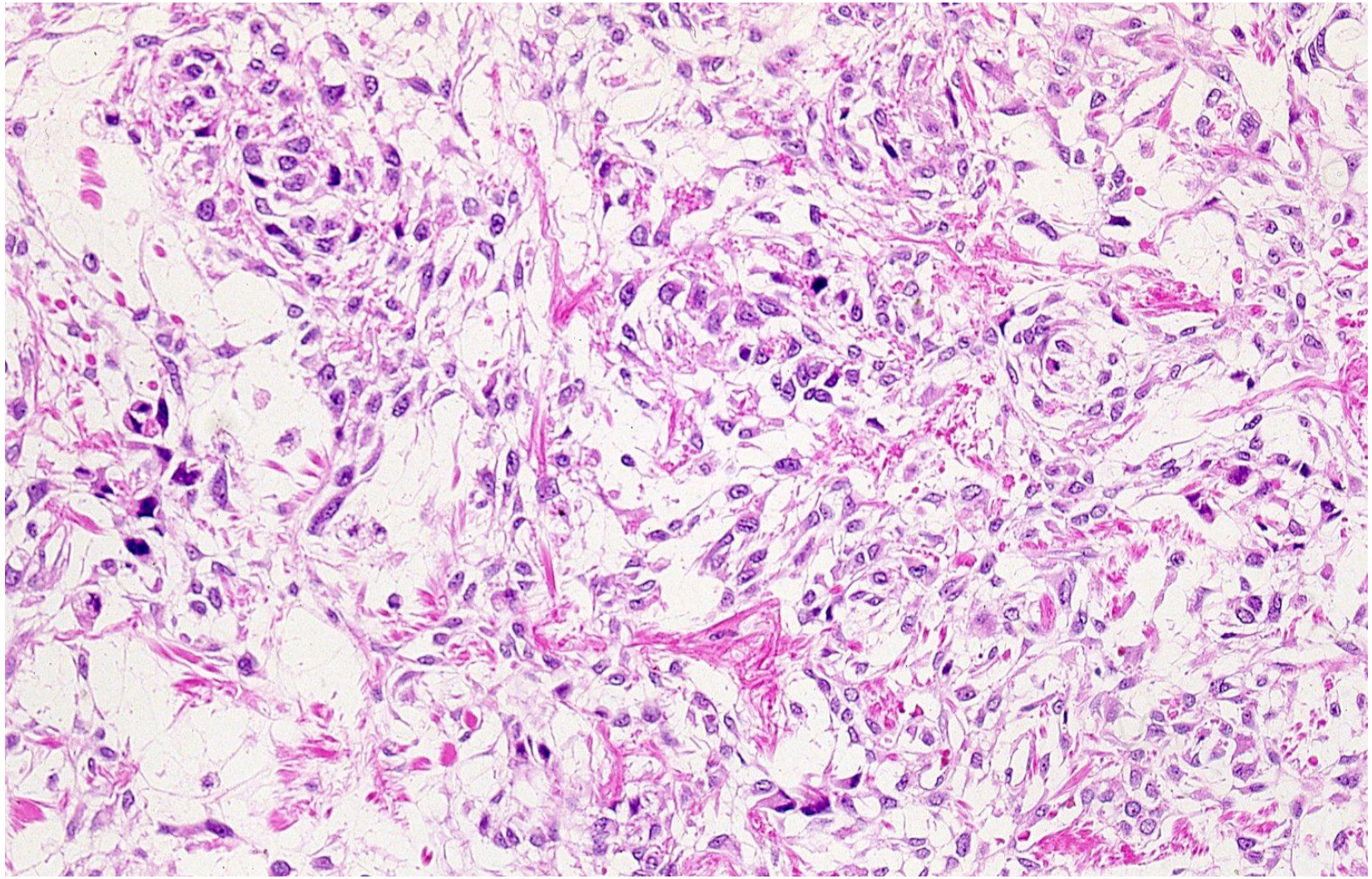

The surgically removed meningioma of the right posterior lobe shows microscopic features of myxoid meningioma (1). The meningioma cells are embedded in the myxoid stroma. H&E

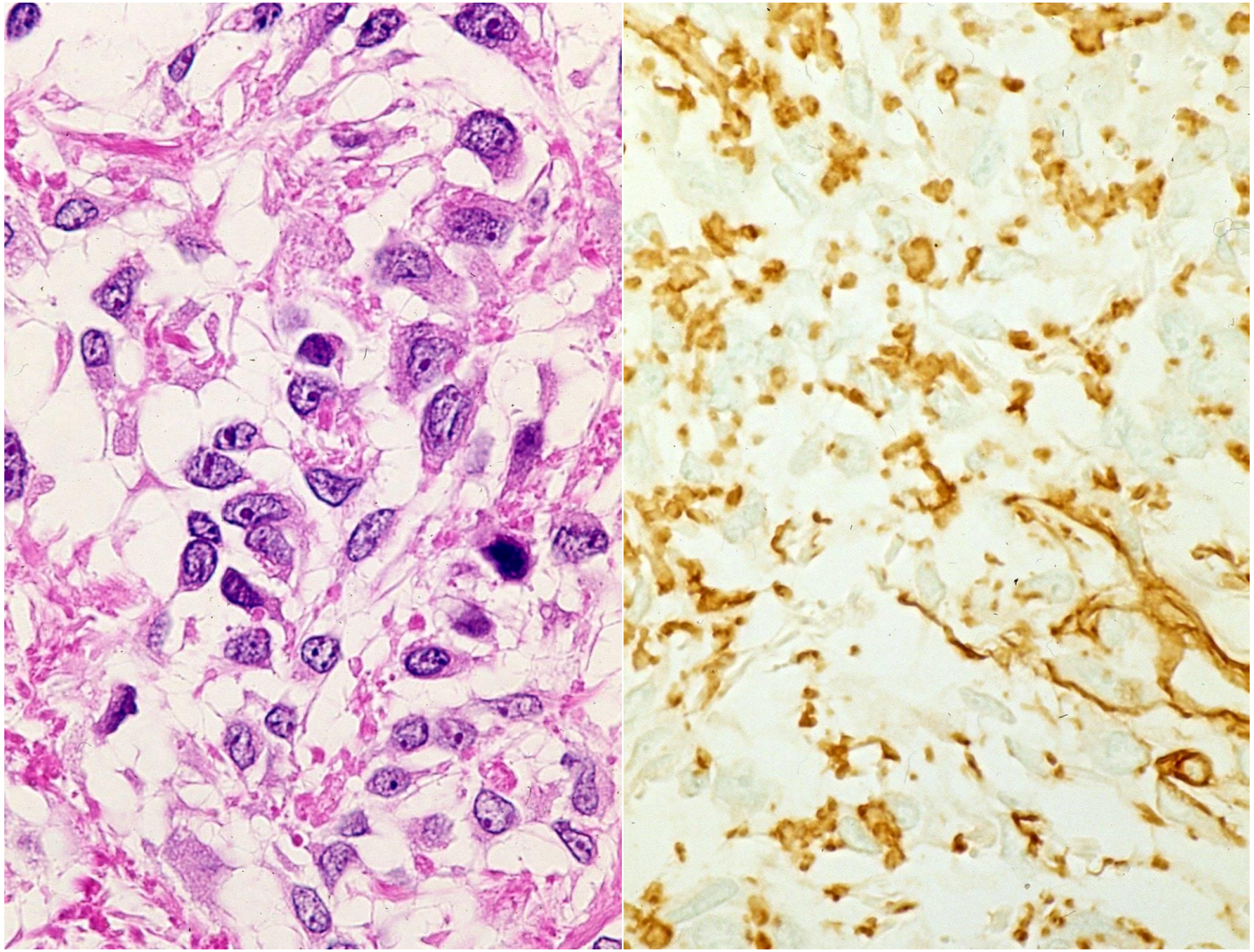

The surgically removed meningioma of the right posterior lobe shows microscopic features of myxoid meningioma (2). The meningioma cells are embedded in the myxoid stroma. Hyaline matrix dispersed in the stroma is immunoreactive for type 4 collagen. (left: H&E, right: immunostaining for type 4 collagen)

Malignant meningioma seen in a 58-year-old female patient (1).
An invasive tumor is located at the left parietal lobe.

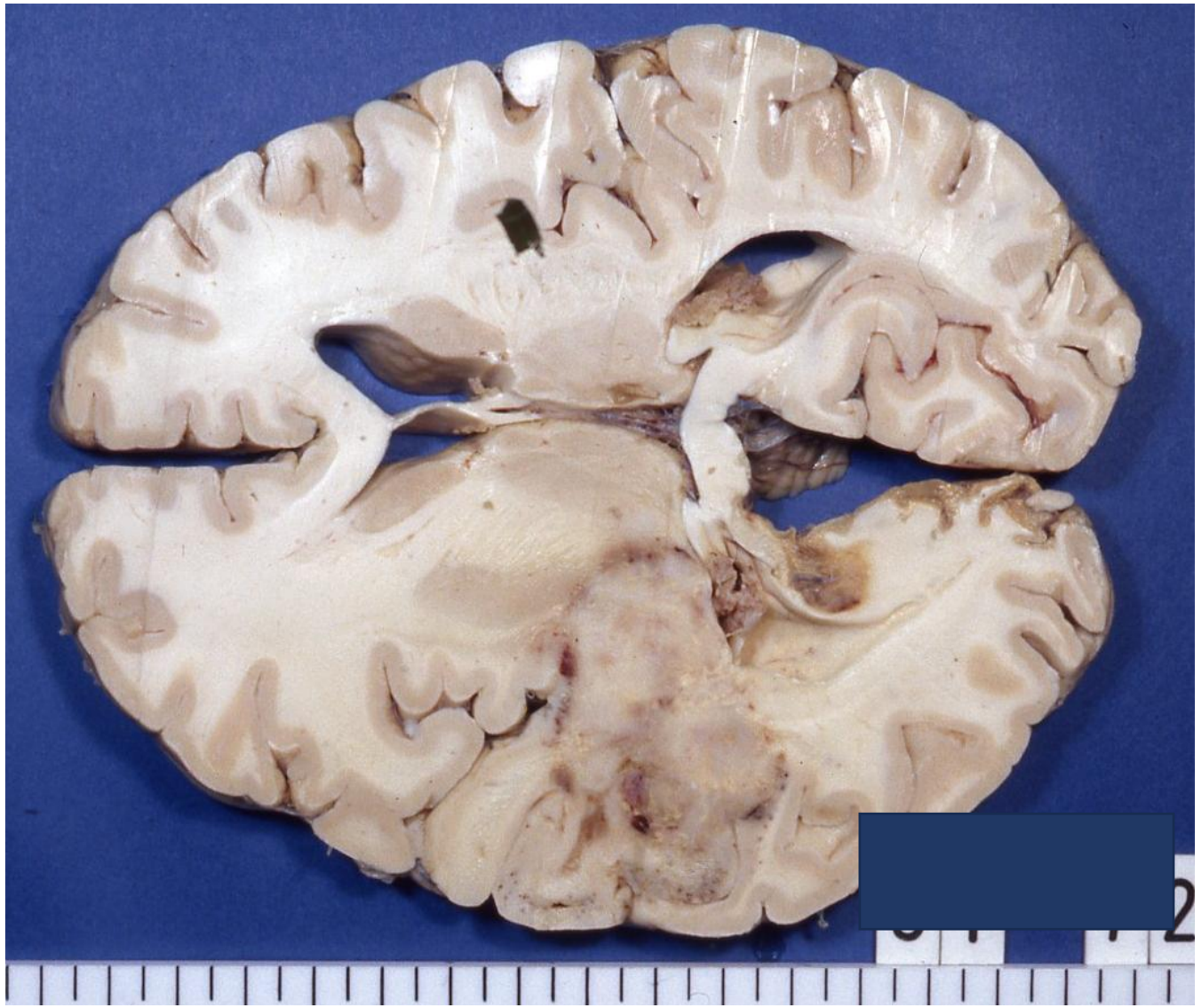

Malignant meningioma seen in a 58-year-old female patient (2). The tumor deeply invades the left parietal lobe, reaching the basal ganglia.

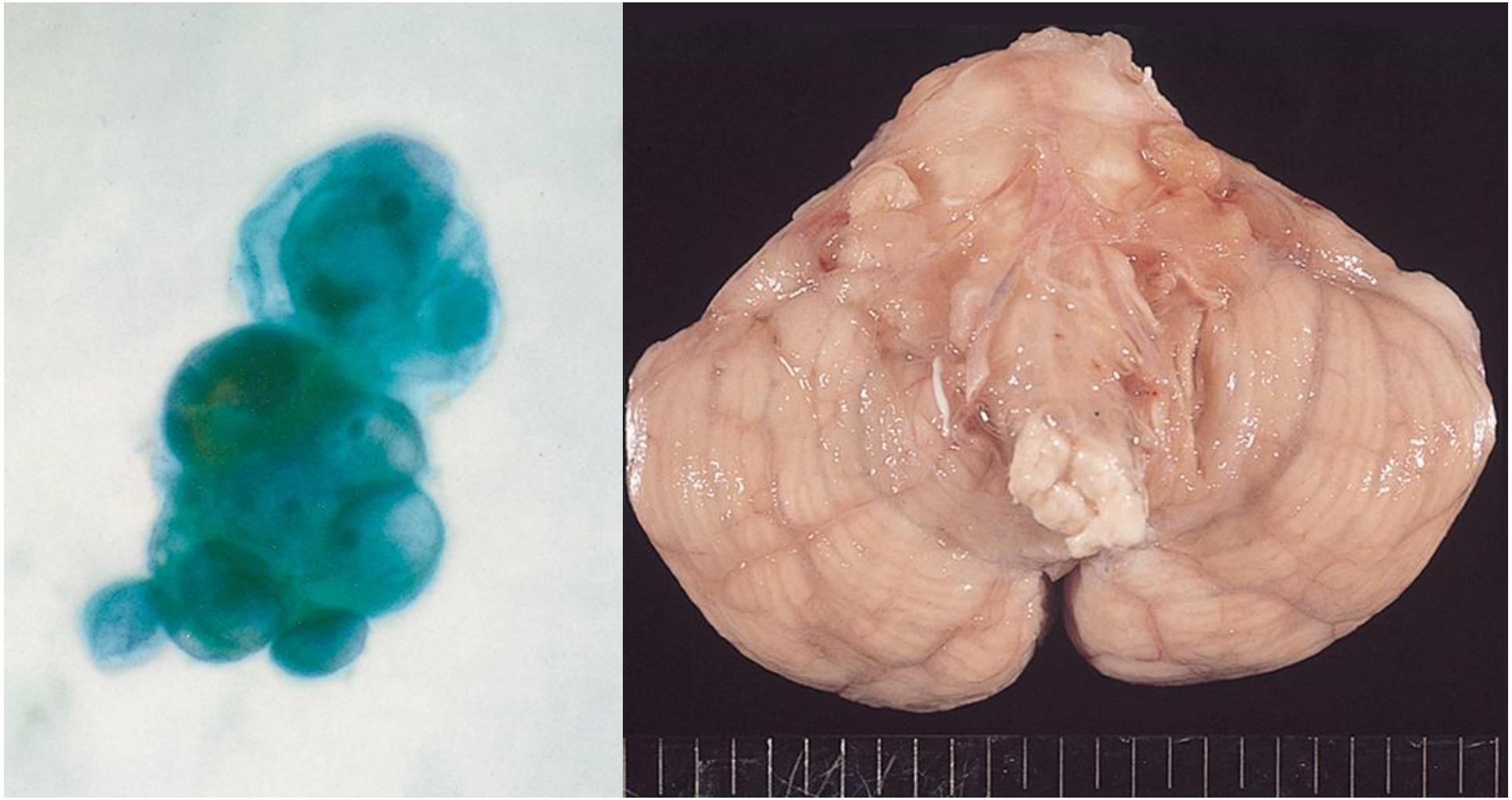

Meningeal dissemination of mucin-producing lung adenocarcinoma (left: cytology of CSF, Papanicolaou, right: gross appearance of the cerebellum). A papillary cluster of mucin-containing adenocarcinoma cells is identified in the CSF. Mucinous appearance of the meninges is grossly quite characteristic.

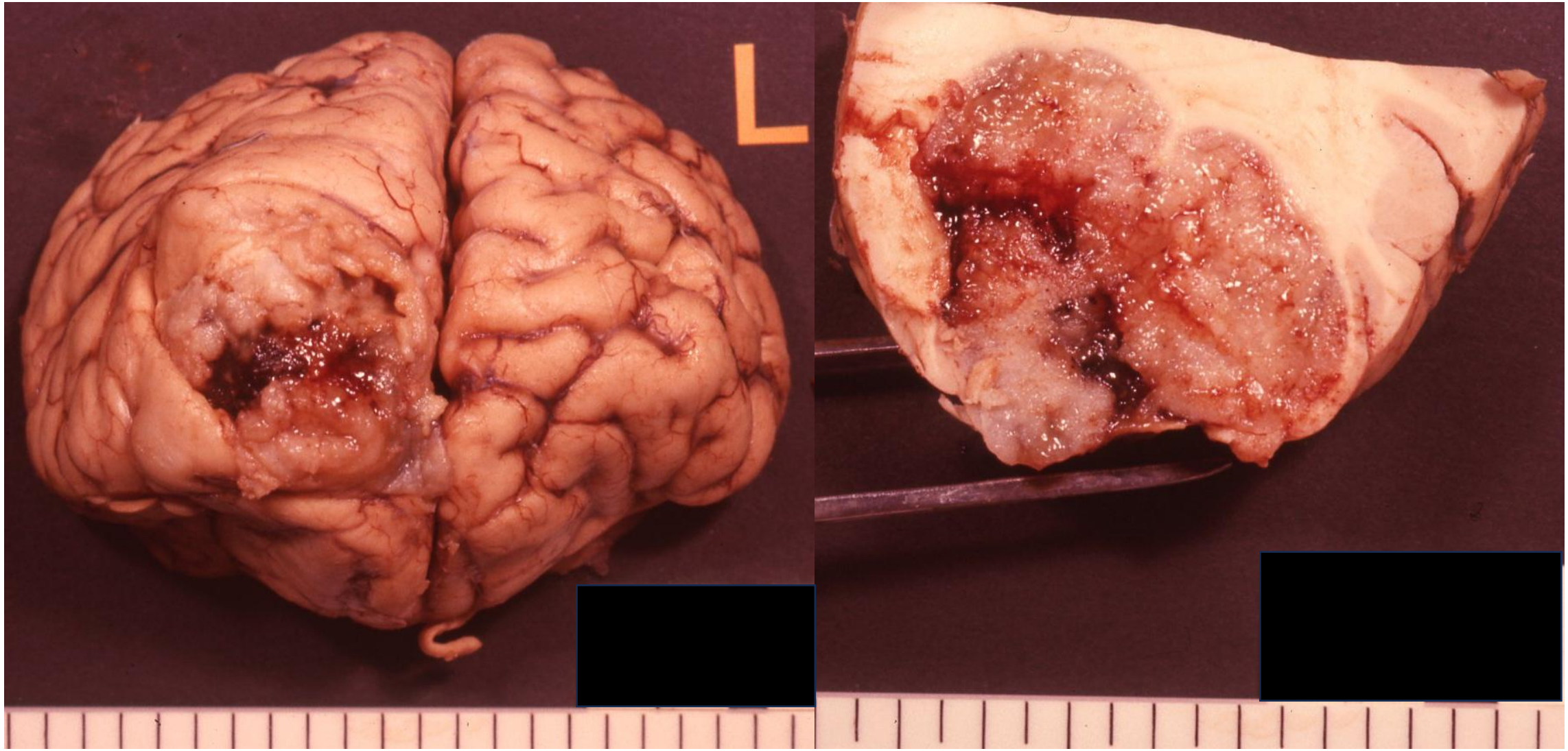

Brain metastasis of mucinous adenocarcinoma of the rectum (a 62-year-old female patient).
A 60 mm-sized mucinous tumor is metastatic to the right frontal lobe.

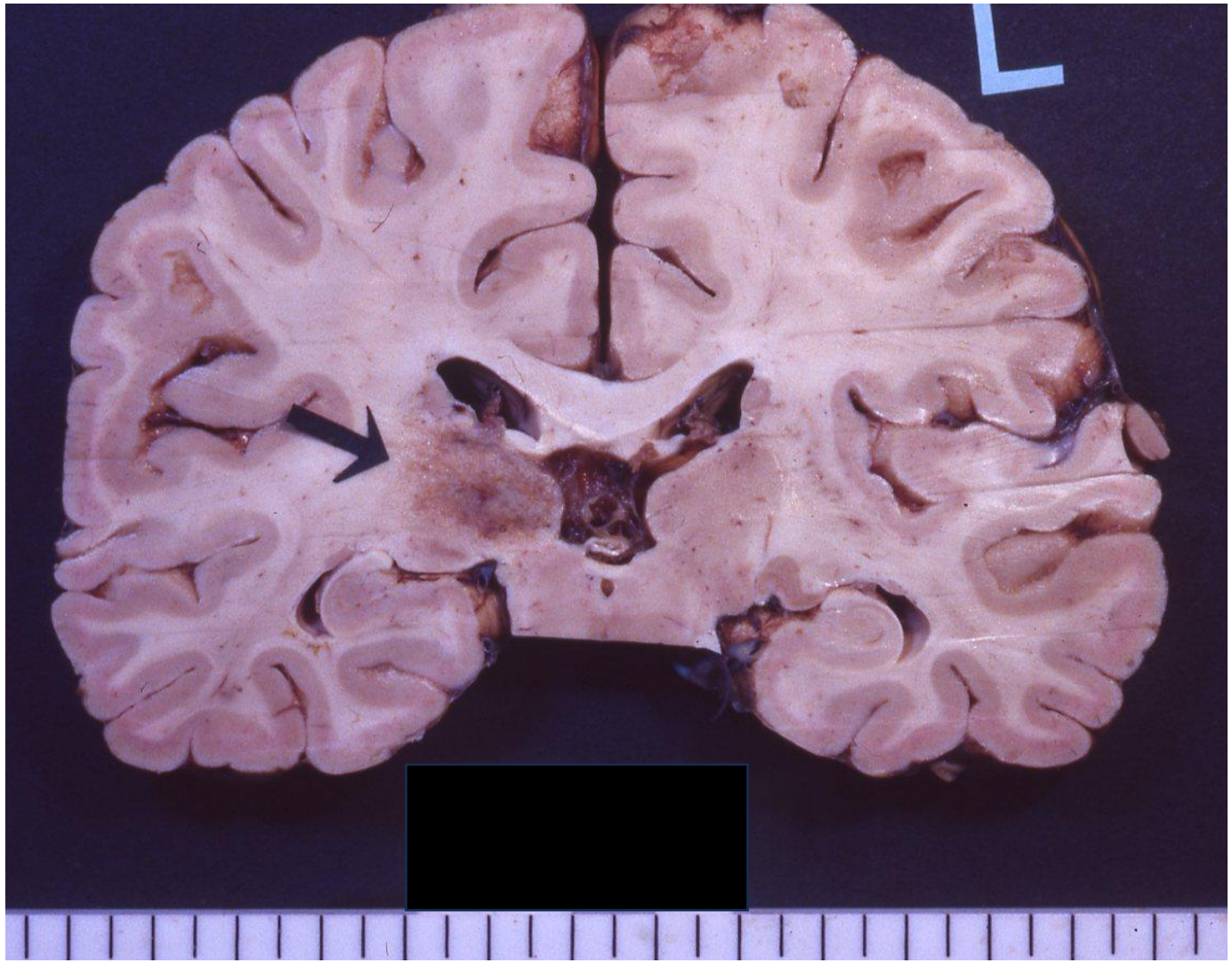

Metastatic lung adenocarcinoma in the right thalamus (arrow).
A female patient aged 60’s.

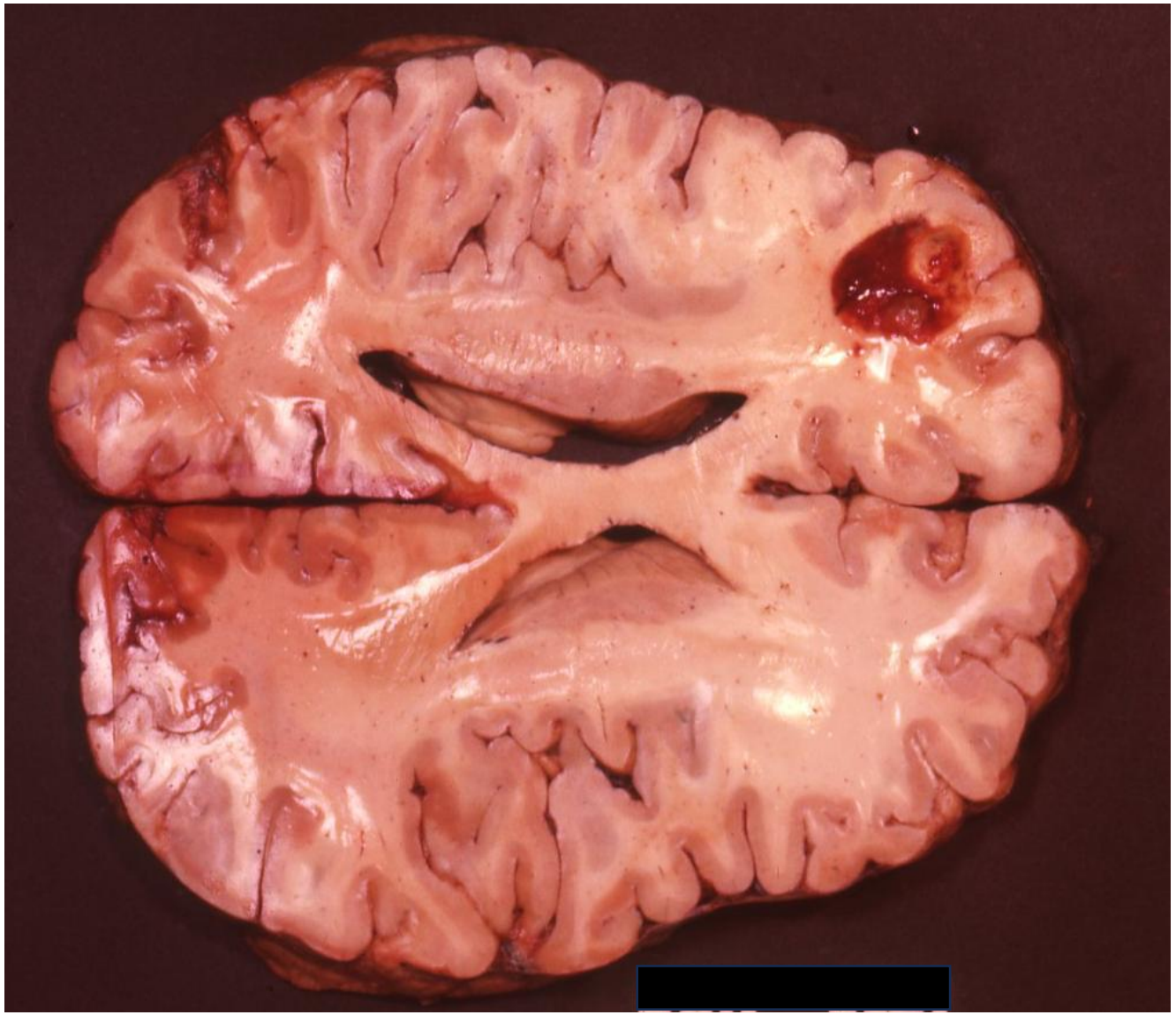

Brain metastasis of papillary thyroid carcinoma in the right frontal lobe. A 55-year-old male patient.